NASA TECHNICAL MEMORANDUM

NASA TM X-62,487

NASA TM X-62,487

A SUBVORTEX TECHNIQUE FOR THE CLOSE APPROACH TO A DISCRETIZED VORTEX SHEET

Brian Maskew

Ames Research Center
Moffett Field, California 94035

September 1975

1. Report No.	2. Government Accession No.	3. Recipient's Catalog No.
TM X-62,487		

4. Title and Subtitle	5. Report Date
A SUBVORTEX TECHNIQUE FOR THE CLOSE APPROACH TO A DISCRETIZED VORTEX SHEET	6. Performing Organization Code
7. Author(s)	8. Performing Organization Report No.
Brian Maskew	A-6277
	10. Work Unit No.
9. Performing Organization Name and Address	505-06-11
NASA Ames Research Center Moffett Field, Calif. 94035	11. Contract or Grant No.
	13. Type of Report and Period Covered
12. Sponsoring Agency Name and Address	Technical Memorandum
National Aeronautics and Space Administration Washington, D. C. 20546	14. Sponsoring Agency Code

15. Supplementary Notes

16. Abstract

The close-approach problem associated with flow calculation methods based on vortex-lattice theory is examined numerically using two-dimensional discretized vortex sheets. The analysis first yields a near-field radius of approximately the distance apart of the vortices in the lattice; only within this distance from the sheet are the errors arising from the discretization significant. Various modifications to the discrete vortices are then considered with the objective of reducing the errors. This study leads to a near-field model in which a vortex splits into an increasing number of subvortices as it is approached. The subvortices, whose strengths vary linearly from the vortex position, are evenly distributed along an interpolated curve passing through the basic vortices. This subvortex technique can be extended to the three-dimensional case and is efficient because the number of vortices is effectively increased, but only where and when needed.

17. Key Words (Suggested by Author(s))	18. Distribution Statement
Vortex lattice theory Close interference	Unlimited STAR Category — 02

19. Security Classif. (of this report)	20. Security Classif. (of this page)	21. No. of Pages	22. Price*
Unclassified	Unclassified	32	$3.75

*For sale by the National Technical Information Service, Springfield, Virginia 22151

A Subvortex Technique for the Close Approach to a Discretized Vortex Sheet

Brian Maskew*

NASA Ames Research Center, Moffett Field, Calif. 94035

The close-approach problem associated with flow calculation methods based on vortex-lattice theory is examined numerically using two-dimensional discretized vortex sheets. The analysis first yields a near-field radius of approximately the distance apart of the vortices in the lattice; only within this distance from the sheet are the errors arising from the discretization significant. Various modifications to the discrete vortices are then considered with the objective of reducing the errors. This study leads to a near-field model in which a vortex splits into an increasing number of subvortices as it is approached. The subvortices, whose strengths vary linearly from the vortex position, are evenly distributed along an interpolated curve passing through the basic vortices. This subvortex technique can be extended to the three-dimensional case and is efficient because the number of vortices is effectively increased, but only where and when needed.

The author wishes to thank Mrs. Opal J. Lemmer for her assistance with the computer programs for this work. He is also grateful to Dr. V. J. Rossow and Messrs. R. T. Medan and V. R. Corsiglia of the Large-Scale Aerodynamics Branch at NASA Ames Research Center; the paper has undoubtedly benefited from their interested discussions during the course of this work and also from their comments on the first draft.

*NRC Research Associate on leave of absence from Hawker Siddeley Aviation Ltd., (Brough), North Humberside, England.

1. Introduction

Velocity distributions calculated close to a discretized vortex sheet show distortions because of the singular behavior of the induced velocity field near each vortex. The problem is associated with all vortex-lattice-based methods (e.g., Refs. 1-5), but it has been circumvented in the past by calculating near-field velocities only at special points, e.g., midway between the vortices, or by interpolation between velocities at nearby "good" points. For calculations involving multiple vortex sheets,[4,5] the near-field problem often requires that adjacent lattices be made to correspond across the gap between the sheets. However, such a solution is not practical for recent developments in vortex-lattice methods which incorporate iterative calculation schemes for trailing vortex relaxation[3,5] (i.e., force-free wake). Although the new methods have proved to be very versatile in general, close-approach situations involving multiple discretized votex sheets require careful treatment, and ideally, the near-field problem should be removed.

The purpose of this investigation, therefore, is to develop a near-field modification for the discrete vortices which will allow velocities to be calculated anywhere in the flow field irrespective of the proximity of discretized vortex sheets. Such a modification would enhance the versatility of vortex-lattice-based methods.

In the investigation, a near-field region is first defined and its extent examined numerically (Sec. 2) before considering two near-field models (Sec. 3) which lead to the subvortex technique. The latter is described in Sec. 4, and an application is given in Sec. 5. The analysis is performed using two-dimensional situations, but the application to the three-dimensional case is taken into consideration in the choice of a suitable model.

2. Extent of the Near-Field Region

In determining the extent of the near-field region, two aspects of the close-approach problem are of interest: 1) How close can a discrete vortex approach a discretized vortex sheet before its lateral position relative to the lattice control points distorts the vorticity solution significantly? 2) How close can a discretized vortex sheet be approached before the calculated velocity distribution shows significant errors? The two aspects are clearly related and would be expected to yield similar near-field criteria, but it is instructive to consider them separately, bearing in mind that both situations can occur in multiple-component calculations with force-free wakes.

For this investigation errors greater than 0.5% will be regarded as significant, i.e., this figure will define the edge of the near-field region here. It is well below current experimental accuracy for velocity measurements.

2.1 Vorticity Solution

To examine aspect (1) of the close-approach problem, consider an infinite discrete vortex situated above and parallel to an infinite plane surface. The flow field is two-dimensional, and the vorticity distribution induced on the surface is:

$$\gamma(y) = -\bar{\Gamma}Z/\pi[(y - Y)^2 + Z^2] \qquad (1)$$

where y is measured along the surface (Fig. 1), (Y, Z) is the vortex location, and $\bar{\Gamma}$ is the vortex strength.

The region $-1.0 \leq y \leq 1.0$ is now discretized using "N" equally spaced vortices. Control points are positioned midway between the discrete vortices (Fig. 1) following standard vortex-lattice procedure. The boundary condition

specified at the control points is that the vortices in the surface induce the same normal velocity as that induced by the replaced part of the vortex sheet:

$$\frac{1}{2\pi} \sum_{i=1}^{N} \frac{\Gamma_i}{y_{c_j} - y_{v_i}} = W(y_{c_j}) \quad ; \qquad i = 1, 2, .., N-1 \tag{2}$$

where $y_{c_j} = j\Delta - 1.0$ are the control points; $y_{v_i} = (i - 0.5)\Delta - 1.0$ are the vortex points; $\Delta = 2.0/N$ is the vortex spacing; and Γ_i are the (unknown) vortex strengths;

and

$$W(y) = -\frac{\bar{\Gamma} Z}{2\pi^2[(y - Y)^2 + Z^2]} \left(\frac{1}{2} \ln \left\{ \left[\frac{(1 - Y)^2 + Z^2}{(1 + Y)^2 + Z^2} \right] \left(\frac{1 + y}{1 - y} \right)^2 \right\} + \left(\frac{y - Y}{Z} \right) \left[\tan^{-1}\left(\frac{1 - Y}{Z} \right) + \tan^{-1}\left(\frac{1 + Y}{Z} \right) \right] \right)$$

The Nth equation concerns the conservation of circulation, i.e., the strengths of the surface vortices must add up to the circulation of the replaced part of the vortex sheet:

$$\sum_{i=1}^{N} \Gamma_i = -\frac{\bar{\Gamma}}{\pi} \left[\tan^{-1}\left(\frac{1 - Y}{Z} \right) + \tan^{-1}\left(\frac{1 + Y}{Z} \right) \right] \tag{3}$$

Using Eqs. (2) and (3) we can solve for the vortex strengths Γ_i and obtain the "discretized" vorticity solution:

$$\gamma_i = \Gamma_i/\Delta$$

In order to keep the edges of the discretized region remote from the region of interest (in terms of vortex spacing), a large number of discrete vortices (N = 40) were used. Solutions were obtained for a range of free vortex locations (Y, Z); at various heights above the sheet the onset vortex

was traversed laterally from a station above a control point to a station above a vortex point.

The calculated vorticity distributions for three heights, $Z = \Delta$, 0.5Δ, and 0.2Δ, are shown in Fig. 2 (centered on the onset vortex lateral position) together with the exact solution from Eq. (1). Appreciable deviations in the solution occur only below $Z = \Delta$. Above that height the vortex position relative to the lattice arrangement is not critical, e.g., at $Z = 2\Delta$ the maximum error in vorticity in the peak region is of the order of 0.001%, while at $Z = \Delta$ it is only 0.37%. With the onset vortex at $Z = 0.5\Delta$ the error near the vorticity peak varies from +10% to -10% as the vortex moves from a point above a control point to one above a vortex point. When the vortex is at either end of the traverse, the vorticity errors decrease with distance from the peak vorticity position and are symmetrical about that point (Fig. 2b). For intermediate locations of the onset vortex, however, the errors are appreciable over a wide region, and they tend to be antisymmetrical about the peak vorticity position. For very small heights, where the solution is tending towards a concentrated vortex, even larger antisymmetric errors appear in the solution unless the vortex lies above a control point or above a vortex point (Fig. 2c).

An interesting observation is that the solution with the vortex above a control point has a positive error, while that for the vortex above a vortex point has a negative error of about the same magnitude. Combining the two solutions at the middle station gives a very small error. It might be possible to make use of this fact in situations where a single vortex is very close to a discretized vortex sheet.

2.2 Velocity Distributions

To evaluate the near-field distance for the velocity calculation aspect, consider a flat, two-dimensional vortex sheet with a parabolic vorticity distribution:

$$\gamma(y) = y(1 - y) \; ; \; 0 \leq y \leq 1$$

The exact induced velocity components are:

$$V(y, z) = \left\{[y(y - 1) - z^2]\, T(y, z) + 2z(0.5 - y)L(y, z) + z\right\}/2\pi$$

$$W(y, z) = \left\{2z(0.5 - y)\, T(y, z) - [y(y - 1) - z^2]L(y, z) + y - 0.5\right\}/2\pi$$

where

$$L(y, z) = \frac{1}{2} \ln\left[\frac{y^2 + z^2}{(y - 1)^2 + z^2}\right]; \quad y \neq 0, \; y \neq 1 \text{ if } z = 0$$

and

$$T(y, z) = \tan^{-1}\left(\frac{y}{z}\right) - \tan^{-1}\left(\frac{y - 1}{z}\right)$$

and V is the velocity component parallel to the vortex sheet; W is the normal component, i.e., in the direction of z.

Now discretize the vortex sheet using "N" equally spaced vortices at locations:

$$y_{v_i} = (i - 0.5)\Delta \; ; \quad i = 1, 2, \ldots, N$$

where $\Delta = 1.0/N$ is the vortex spacing.

Integrating the vorticity over each vortex region yields the vortex strengths:

$$\Gamma_i = y_{v_i}(1.0 - y_{v_i})\Delta - (\Delta^3/12); \quad i = 1, 2, \ldots, N$$

The velocity components induced by the discretization are:

$$V_d(y, z) = -\frac{1}{2\pi} \sum_{i=1}^{N} \frac{\Gamma_i z}{\left[\left(y - y_{v_i}\right)^2 + z^2\right]}$$

$$W_d(y, z) = \frac{1}{2\pi} \sum_{i=1}^{N} \frac{\Gamma_i \left(y - y_{v_i}\right)}{\left[\left(y - y_{v_i}\right)^2 + z^2\right]}$$

Using forty discrete vortices, velocity distributions were calculated over a region between two midpoints near the quarter position on the segment (Fig. 3a). Error contours are shown in Fig. 3b. The discretization gives negligible errors for both components of velocity in the region beyond 1Δ from the sheet. In effect the "holes" in the representation are not sensed until we enter the 1Δ region.

Inside the 1Δ region the errors increase rapidly except along special lines of approach to the sheet. For the normal velocity component, the zero-error lines follow approximately the normals to the sheet at the points midway between the vortices and also at the vortices. (Deviations from the normal lines occur because of the gradient in vorticity across the region.) Both sets of positions on the surface are used in the extended vortex-lattice method,[5] i.e., the midpoints are used as control points, as in the standard vortex-lattice theory, and the vortex points are used when applying the Kutta-Joukowski law for local forces and also when performing the trailing-vortex roll-up calculations. The zero-error lines for the tangential velocity component are less well known; these lines enter the near-field region above the quarter and three-quarter positions between the vortices and approach the vortex locations along approximately elliptical paths. All the zero-error paths are situated on extreme "precipices" in the error contour map; small deviations from the paths result in large errors and lead to the near-field problems.

3. Near-Field Models

The previous section indicates that errors arising from the discretization of a vortex sheet become appreciable only within the 1Δ region. Clearly, if we wished to calculate velocities very close to the discretized vortex

sheet, we could simply decrease the size of Δ by increasing the number of vortices; however, for three-dimensional problems the computing time could then become prohibitive. An alternative solution is to apply a near-field treatment to the vortices. This treatment would be applied only to those vortices that are within a specified "near-field radius" (e.g., 1Δ) from the point where the velocity is being calculated. A number of near-field models were considered in this work in two groups, i.e., "core-models" and "spread-models." The distinguishing feature between the groups is that whereas core models are applied without reference to neighboring vortex positions, spread models require that information to generate connecting "vortex sheets." One model from each group is described in this section. These lead to the sub-vortex technique, which is described separately in Sec. 4.

3.1 Core Models

A core model offers the simplest near-field treatment which removes the singular behavior of the velocity field. In such a model the velocity induced by the vortex is factored locally so as to remain bounded at the vortex center. The Rankine Vortex and Lamb's viscous vortex are well known examples, but there are other possible forms. Core models have been used in the past to smooth the motions of vortices used in two-dimensional roll-up calculations (e.g., Refs. 6 and 7).

Several core models were tested using the discretized parabolic vorticity sheet from Sec. 2.2, but none were found satisfactory for both components of velocity. For example, they fail to restore the tangential component of velocity near the vortex sheet. This can be seen in Fig. 3c(i) which shows the error contours for a Rankine vortex model with a core diameter of Δ. Although the tangential velocity errors appear slightly worse than for the unmodified vortex [compare Figs. 3c(i) and 3b], the normal component errors

are improved on the whole within the core. But the error levels are still significant, and the zero-error lines no longer approach the vortex points.

3.2 Spread Models

In spread models the vortex itself is modified, and its strength is effectively distributed along a line representing the local position of the vortex sheet. Compared with core models, spread models would be more difficult to apply to the three-dimensional case and would be expected to consume more computing time.

There are a number of ways of spreading the strengths of the vortices; one based on a linear distribution of vorticity proved very effective. In this model the vorticity associated with a vortex is distributed in a triangular fashion on the two straight segments joining the vortex to its immediate neighbors. When several neighboring vortices are treated in this way, the local effect is that of a piecewise, linear distribution of vorticity—a model already known to work well in two-dimensional aerofoil theory (e.g., Ref. 5).

When evaluating this model on the discretized parabolic vorticity distribution from Sec. 2.2, it was found necessary to extend the near-field radius of the vortices from 1Δ to 4Δ to achieve the required accuracy. (The larger radius is required only for the lateral distance along the sheet; it is not required for the normal distance from the sheet, which is still 1Δ.) The reason for the extended radius will be discussed in Sec. 4.2.

With the larger near-field radius, the errors for this problem are less than 0.5% everywhere in the flow field, including the surface of the vortex sheet. However, the three-dimensional form of this model can be cumbersome to apply in a general method. A discretized form of this model was therefore considered, and this formed the basis of the subvortex technique.

4. Subvortex Technique

In the subvortex technique, the spreading of a near-field vortex is achieved by splitting it into a number of small vortices which are placed between the basic vortex positions. The technique offers a number of advantages over the linear vorticity model and has several novel features.

4.1 Features of the Technique

(a) Subvortex positions

The subvortices are distributed evenly along the vortex sheet joining the vortex to its two immediate neighbors. Unlike the linear vorticity model considered in Sec. 3.2, the joining sheet is not necessarily a straight line; the subvortices can be placed on an interpolated curve passing through the basic vortices, and so a better representation of curved vortex sheets is possible. Half intervals separate the basic vortices from the nearest subvortices (Fig. 4a), and so the basic vortex positions become midpoints in the subvortex system. This feature improves the accuracy of the calculated velocity at the basic vortices (see Sec. 4.3).

(b) Number of subvortices

The number of subvortices used is such that the point where the velocity is being calculated cannot "see the holes" in the discretized vortex sheet, i.e., the point is kept just outside the new local 1Δ region of the subvortex system. Figure 4b shows how this works using the following expression for the number of subvortices on one side of the basic vortex:

$$NSV = \text{integer-part-of } (1 + \Delta/H) \tag{4}$$

where H is the normal distance of the point from the segment. Use of this expression keeps the number of subvortices to a minimum and helps to keep computing costs down. When applied to the vortex-lattice methods, the midpoints between the vortices (i.e., the control points) should remain

midpoints in the subvortex system; NSV must then be even, i.e., as shown dotted in Fig. 4b.

A maximum limit NSV_{MAX} is placed on the number of subvortices to avoid a runaway condition when the height H approaches zero. This limit controls the closest approach that can be made to the vortex sheet before the new local 1Δ region of the subvortices is entered. It can therefore be used to control the "accuracy" of the calculation in a trade-off with computing time, i.e., by increasing the limit the error region would decrease in size, but the computing time would increase, and vice-versa.

(c) Subvortex strengths

The subvortices must have a combined strength equal to that of the associated basic vortex. In the technique as used here their strengths vary linearly with distance from the basic vortex position. With equal spacing, therefore, the ith subvortex has strength

$$\Gamma_i = \frac{\bar{\Gamma}}{(NSV)^2}\,(i - 0.5) \quad ; \quad \text{for } i = 1, 2, \ldots, NSV \text{ on each side of the basic vortex, Fig. 4a.}$$

where $\bar{\Gamma}$ is the strength of the basic vortex. When several neighboring basic vortices are treated in this way, the local effect approaches that of a piecewise linear vorticity distribution. Clearly, higher order distributions could be used but would involve more than one basic vortex interval on each side.

(d) Subvortex cores

Because of the practical limit NSV_{MAX} placed on the number of subvortices, it is possible for a point where the velocity is calculated to fall within the (reduced) 1Δ region of the subvortex system. Because of this each subvortex has been modified with a Rankine-Vortex core (Sec. 3.1) of diameter approximately equal to the distance between the subvortices. This smears out

the discontinuity associated with the sheet but only over the new, diminished, near-field region.

An alternative, but more complicated possibility when a subvortex near-field region is entered is to apply a special "sheared core." For this the velocity point is physically moved the small distance to the nearest midpoint between subvortices when evaluating the local contribution. The usual velocity calculation then provides the local mean velocity, to which is added the local vorticity contribution. The latter is half the local vorticity value (evaluated by dividing the nearest subvortex strength by the subvortex spacing) and is directed along the local tangent on one side of the vortex sheet and in the opposite direction on the other side. A similar sheared core was one of the models tried earlier (Sec. 3.1) but was not satisfactory for the broad intervals of the basic vortices; however, it should improve the subvortex technique.

(e) Extension to three dimensions

The subvortex technique can be adapted to the segmented vortices used in vortex-lattice-based methods. The location of the ends of each subvortex segment is a simple extension of the two-dimensional method.

4.2 Near-Field Radius

As in the case of the linear vorticity model (Sec. 3.2), when testing the subvortex technique, the near-field radius had to be increased beyond 1Δ to obtain the required accuracy. The reason for this extension is that the induced velocity from the "distributed" model does not match that from the basic vortex until some distance away. For the subvortex model this result is fairly insensitive to the number of subvortices (see Fig. 5). Thus, when one vortex has the near-field modification applied, several neighboring vortices must also be modified, otherwise small "jumps" occur in the calculated velocity

distribution as we pass over the near-field boundary of each vortex. These jumps can be made as small as we please by increasing the near-field radius. For the subvortex technique the jumps are effectively eliminated when using a near-field radius of 5Δ.

Although the near-field radius of 5Δ is strictly required only in the direction parallel to the vortex sheet (the normal distance is still 1Δ), a true radius of 5Δ is now used. This can result in superfluous calculations if the point actually lies beyond 1Δ from the sheet, but it does provide more reliable conditions for highly curved vortex sheets. The possible penalty in computing time is alleviated by the fact that the tangential distance between the point and the segment is no longer required and that only a small number of subvortices are used for the outer region, i.e., the region 1Δ to 5Δ (Fig. 4b).

4.3 Error Contours

The technique was tested on the discretized parabolic vorticity distribution considered in Sec. 2.2. The error contours (Fig. 3c(ii)) appear not quite as good as those for the linear vorticity model (Sec. 3.2); a small region with significant error is indicated very close to the vortex sheet where the approach is closer than the subvortex spacing and is associated with the maximum limit placed on the number of subvortices (Sec. 4.1b). In these calculations NSV_{MAX} was 10.

The normal component of velocity calculated at the vortex locations has always been slightly less accurate than that calculated at points midway between the vortices. (The vortex points are effectively midpoints in a coarser discretization.) For the present discretized parabolic vorticity distribution, the error at the vortices in the region considered (see Fig. 3a) is 2.8% compared with 0.03% at the midpoints. With the subvortex technique

applied, the error at the vortices decreases to 0.2%; this reduction is helped by the fact that the basic vortex locations become midpoints in the subvortex system (Sec. 4.1a).

5. Two-Dimensional Application

For a more general situation the subvortex technique was applied to the two-dimensional, time-dependent, roll-up calculation of the vortex sheet shed from a wing with elliptical load distribution:

$$\gamma(y) = 2y/\sqrt{1 - y^2} \; ; \quad -1 < y < 1$$

This problem has been considered by a number of authors, e.g., Refs. 6-8 (most recently). The vortex sheet is first discretized then the motion of the discrete vortices under their mutual interactions is followed over a number of small time steps δt. After the ith time step a point on the trajectory of a vortex is calculated here using the expression

$$\underline{r}_{i+1} = \underline{r}_i + \delta t \, \underline{V}_i$$

where $\underline{V}_i$ is a mean velocity calculated at a midpoint in the time interval. This point is obtained by extrapolating the conditions at the two previous time steps. Before calculating $\underline{V}_i$ all the vortices are moved to their midpoint positions. Unlike most previous roll-up calculations, the influence of the vortex on itself is not ignored here; because the vortex point is a midpoint in the subvortex system (Sec. 4.1a), the vortex can now influence itself if the vortex sheet is curved or stretched locally.

In the present calculation ten equally spaced vortices are used on one half of the sheet, and the time step δt is 0.075. (This is smaller than the shortest orbital period of the vortex pairs in the system (see Ref. 8), that value being 0.2 here.) The vortex positions are shown in Fig. 6a after twenty time steps, i.e., after a time of 1.5. The curve drawn through the

vortex locations is the interpolated curve on which the subvortices are placed. With so few vortices in the roll-up region, interpolation there is difficult; the scheme used here is based on a linear combination of two circular arcs over each interval, but even this breaks down (i.e., crosses itself) after a few more time steps beyond that shown. (When developing the three-dimensional version of the model, such problems will be alleviated by the use of a vortex-amalgamation technique, such as that used by Moore.[8])

Having obtained a representative distribution of discrete vortices, a velocity scan was taken through the roll-up region at $y = 0.8$. The two velocity components are shown in Fig. 6b, c with and without the subvortex technique being used. The basic discretization (with small Rankine-vortex cores applied) shows the characteristic velocity deviations near the discrete vortices and ignores the presence of connecting vortex sheets. Qualitatively, the subvortex technique shows a plausible modeling of the discontinuities associated with the (inviscid) vortex sheet. By increasing the limit on the number of subvortices NSV_{MAX} (from the ten used here), the representation of the discontinuities would be sharpened. Quantitative comparisons are still required for a general case, but these will be pursued after the technique has been incorporated in a three-dimensional method.

The end vortex near the center of the roll-up region requires further treatment, possibly in the form of a viscous core; such a treatment coupled with the amalgamation technique mentioned earlier should improve the calculations near a roll-up region.

6. Conclusions

Discretization of a vortex sheet introduces significant velocity errors only within a distance from the sheet equal to the vortex spacing in the

lattice. Core models applied to the vortices help to limit the size of errors but do not reduce them to a satisfactory level when the field of interest approaches close to the vortex sheet. The region where significant errors occur can be reduced to a small region of controllable width close to the vortex sheet by the use of the near-field model in which a discrete vortex splits into an increasing number of subvortices as it is approached. The two-dimensional problems considered here demonstrate that the subvortex technique can achieve the objective of this investigation, viz., to provide accurate velocities anywhere in the flow-field irrespective of the proximity of discretized vortex sheets. (Clearly, quantitative comparisons with experimental results are still required, but these will be pursued after the model has been incorporated in a three-dimensional method.)

In summary, the subvortex technique promises to enhance the versatility of vortex-lattice-based methods by providing the effect of a much finer discretization. The technique is efficient because the number of vortices in the lattice is effectively increased but only where and when needed and by an amount just sufficient to prevent the "holes" in the lattice from being "seen."

References

[1]Rubbert, P. E., "Theoretical Characteristics of Arbitrary Wings by a Non-Planar Vortex Lattice Method," D6-9244, 1964, Boeing Co., Seattle, Wash.

[2]Giesing, J. P., "Lifting Surface Theory for Wing-Fuselage Combinations," DAC 6712, 1968, McDonnel Douglas Corp., Longbeach, Calif.

[3]Belotserkovskii, S. M., "Calculation of the Flow Around Wings of Arbitrary Planform over a Wide Range of Angles of Attack," TTF-12,291, May 1967, NASA.

[4]Maskew, B., "Calculation of the Three-Dimensional Potential Flow around Lifting Non-Planar Wings and Wing-Bodies using a Surface Distribution of

Quadrilateral Vortex-Rings," TT7009, Sept. 1970, Loughborough University of Technology, Leics, England.

[5]Maskew, B., "Numerical Lifting Surface Methods for Calculating the Potential Flow about Wings and Wing-Bodies of Arbitrary Geometry." Ph.D. Thesis, Oct. 1972, Department of Transport Technology, Loughborough University of Technology, Leics, England.

[6]Chorin, A. J. and Bernard, P. S., "Discretization of a Vortex Sheet with an Example of Roll-up," FM-72-5, Nov. 1972, College of Engineering, University of California, Berkeley, Calif.

[7]Kuwahara, K. and Takami, H., "Numerical Study of Two-Dimensional Vortex Motion by a System of Point Vortices," *Journal of The Physical Society,* Japan, Vol. 34, No. 1, Jan. 1973, pp. 247-253.

[8]Moore, D. W., "A Numerical Study of the Roll-up of a Finite Vortex Sheet," *Journal of Fluid Mechanics,* Vol. 63, Pt. 2, 1974, pp. 225-235.

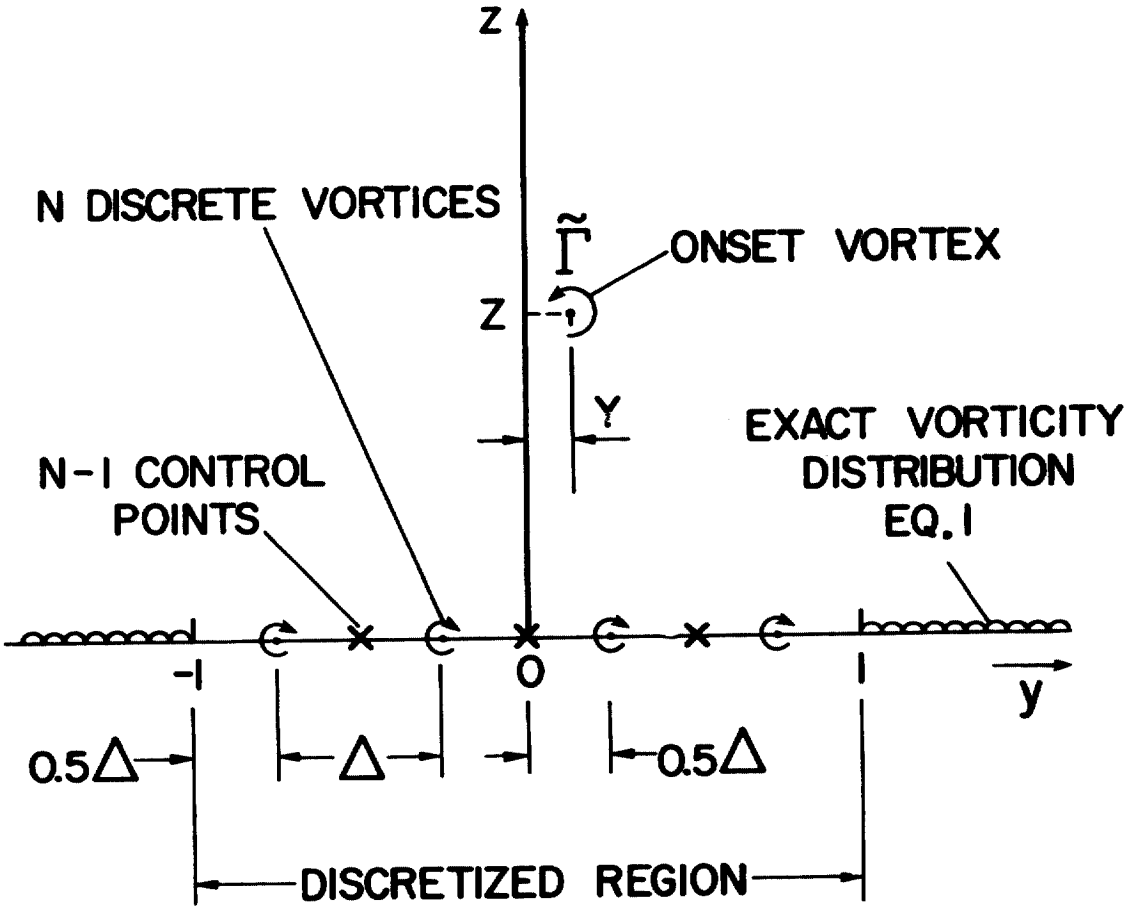

Figure 1.- Vorticity induced on a plane surface by a vortex — discretized model.

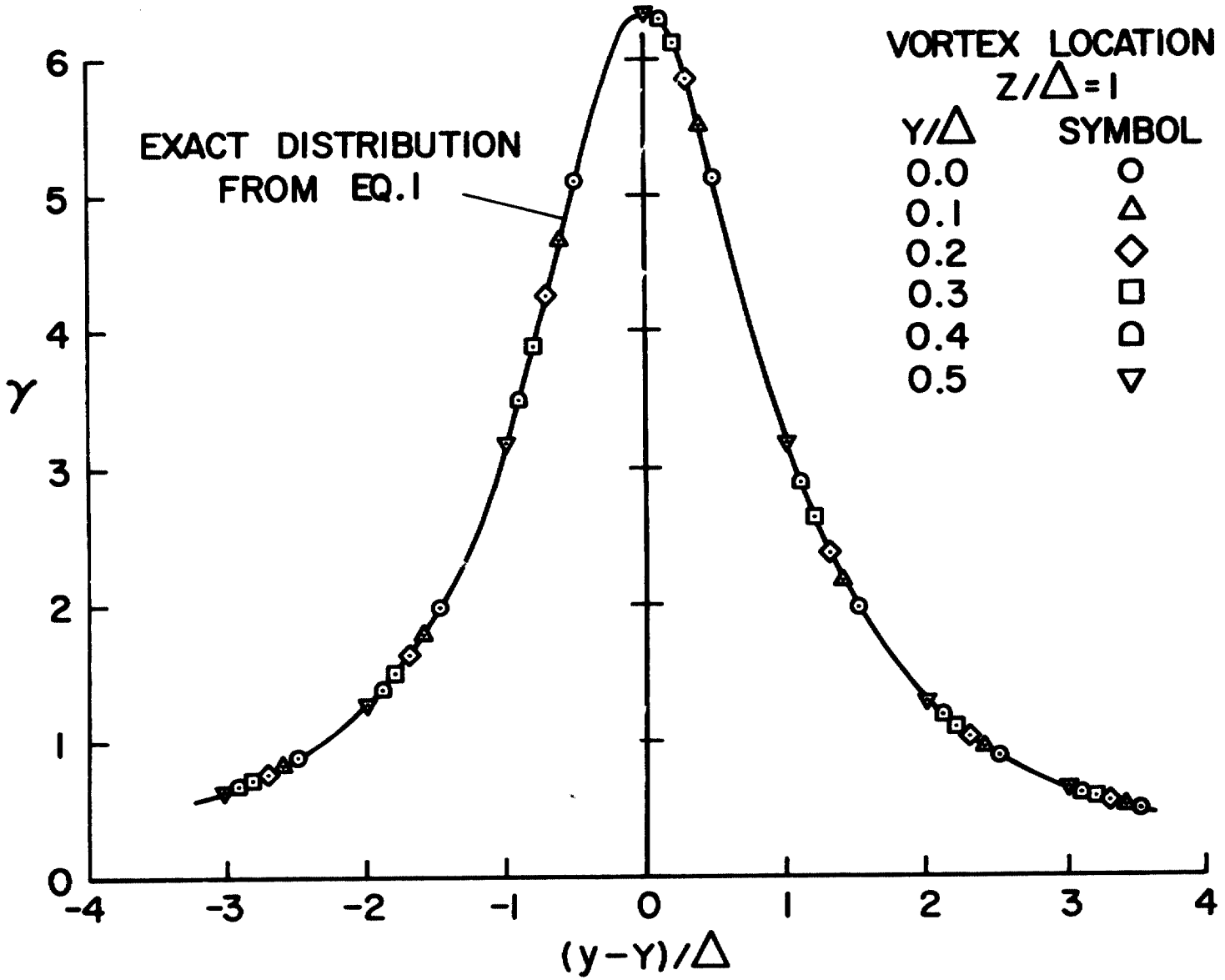

(a) Vortex height, Z = Δ.

Figure 2.- Vorticity induced on a plane surface by a vortex — effect of vortex location on discretized solution.

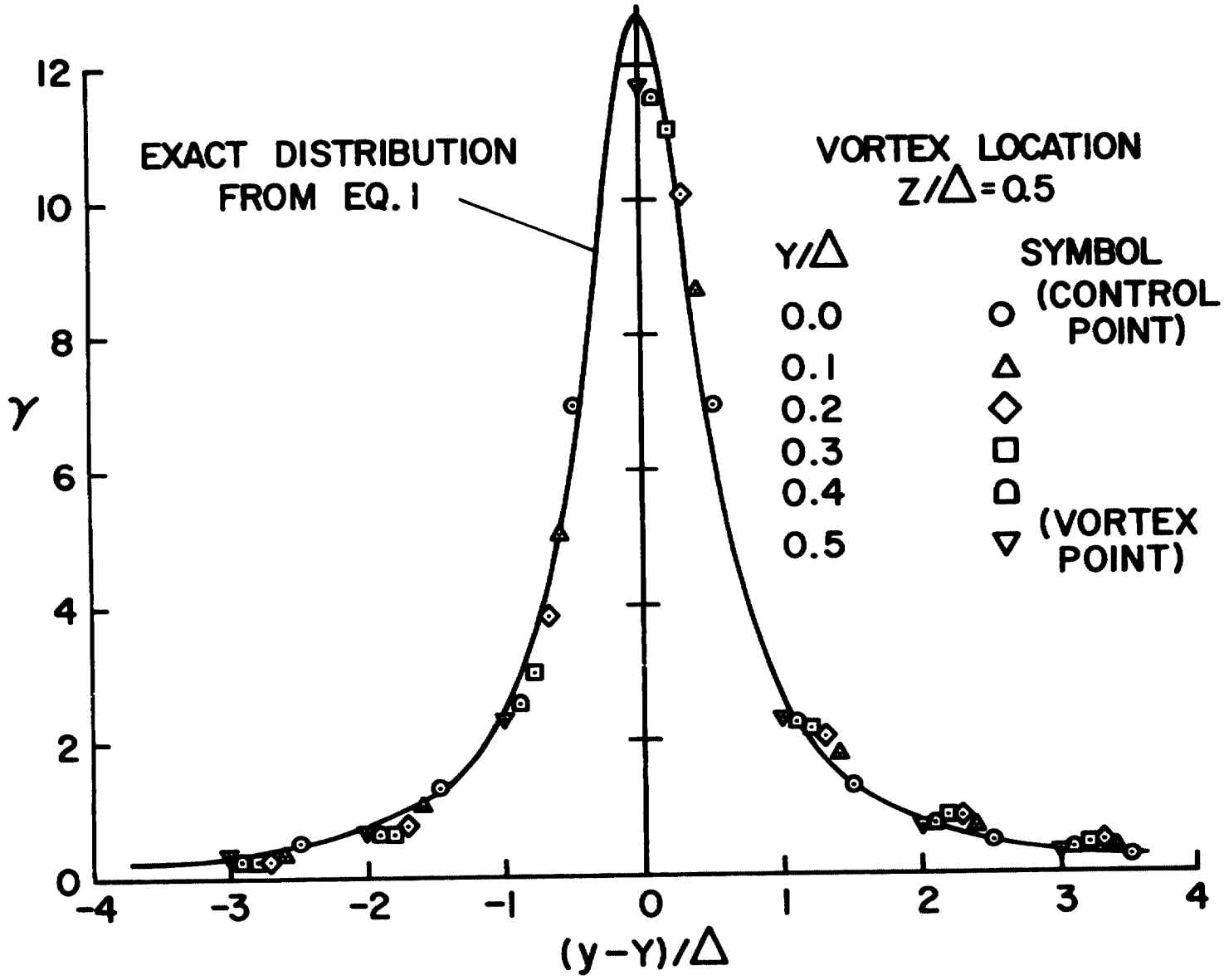

(b) Vortex height, Z = 0.5Δ.

Figure 2.- Continued.

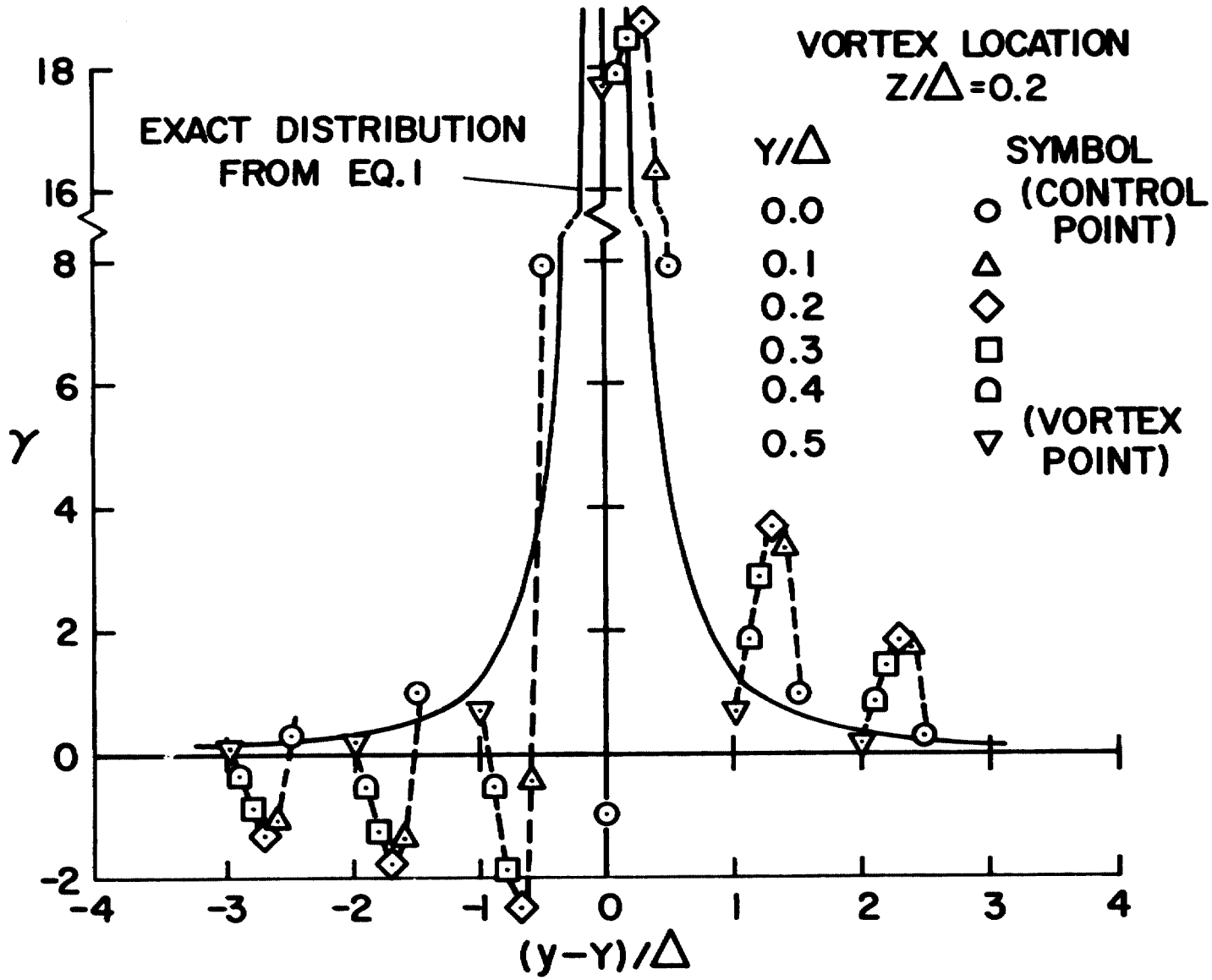

(c) Vortex height, Z = 0.2Δ.

Figure 2.- Concluded.

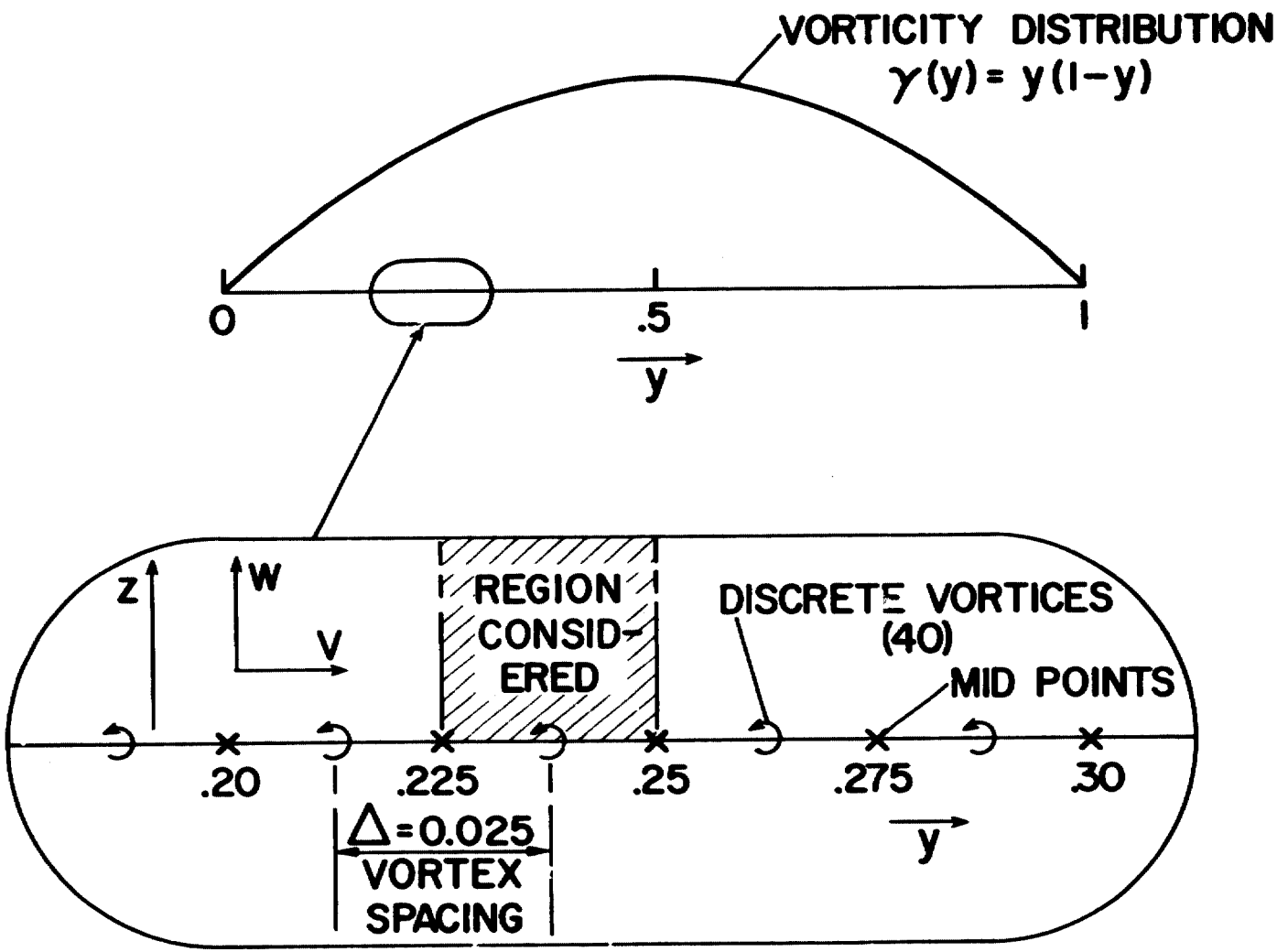

(a) Location of region considered.

Figure 3.- Velocity error calculations.

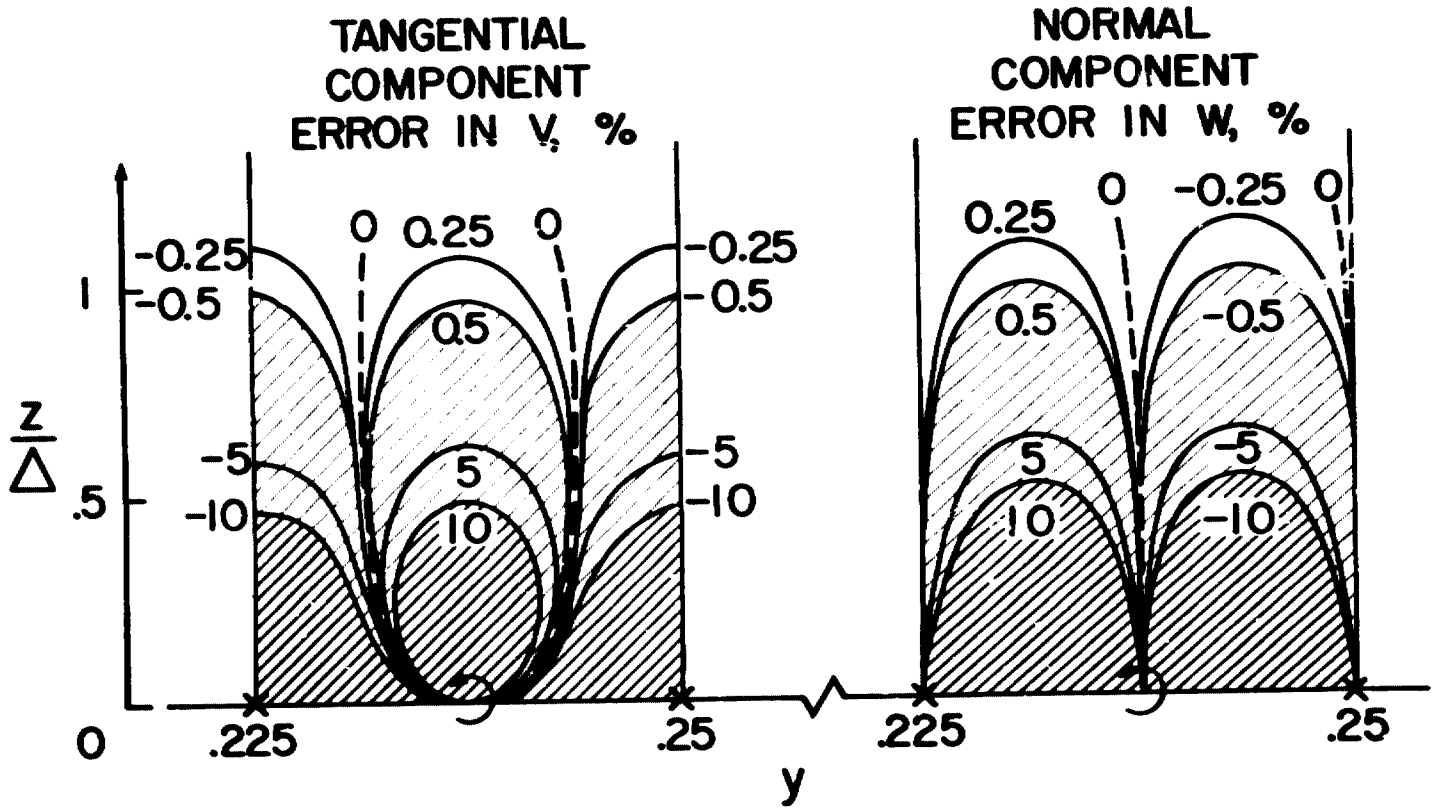

(b) Error contours for the basic discretization.

Figure 3.- Continued.

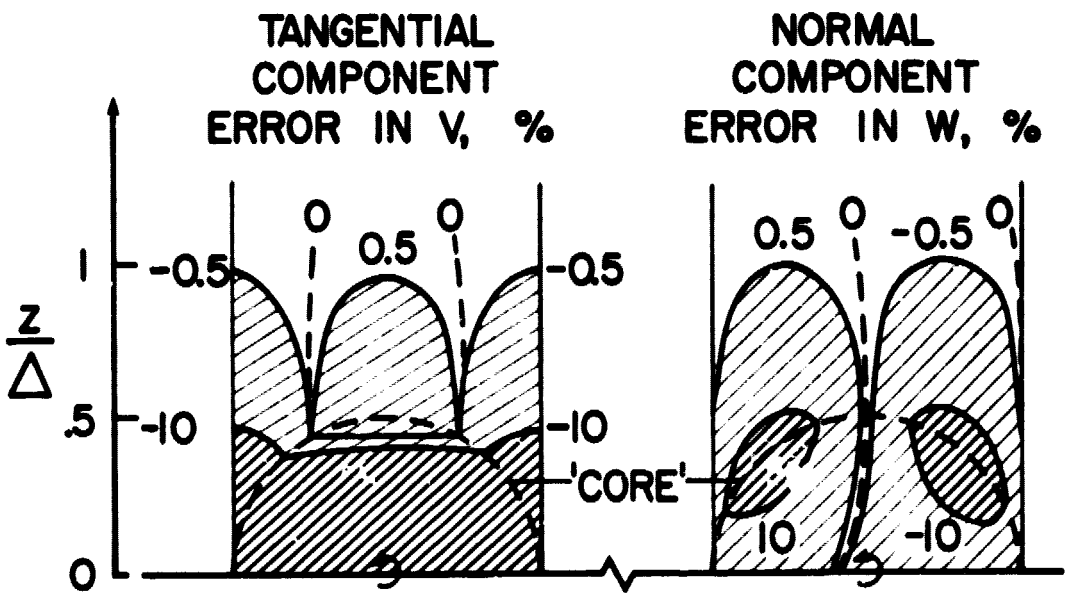

(i) Core model (Rankine vortex); core diameter = Δ.

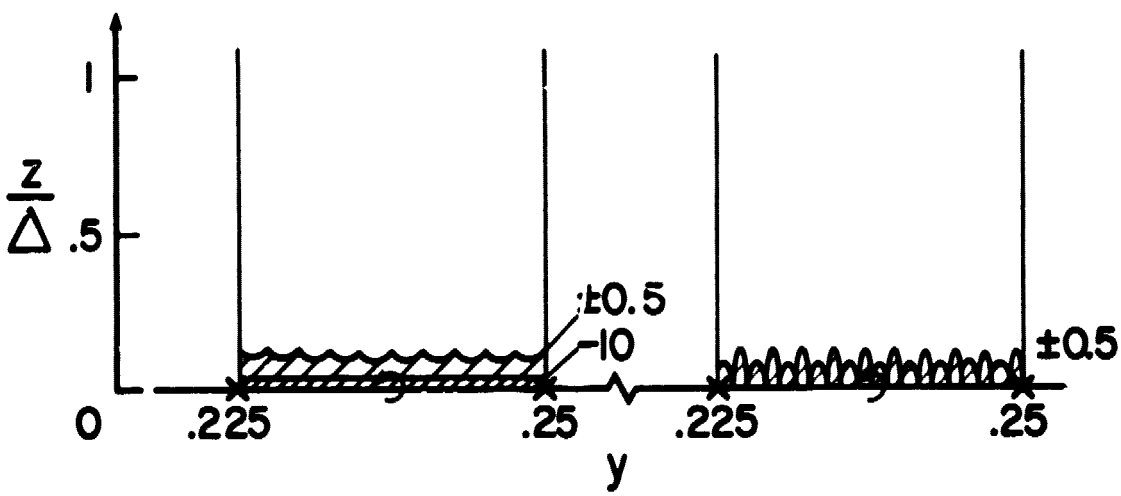

(ii) Subvortex technique; near-f d radius = 5Δ, NSV_{max} = 10.

(c) Error contours for two near-field models.

Figure 3.- Concluded.

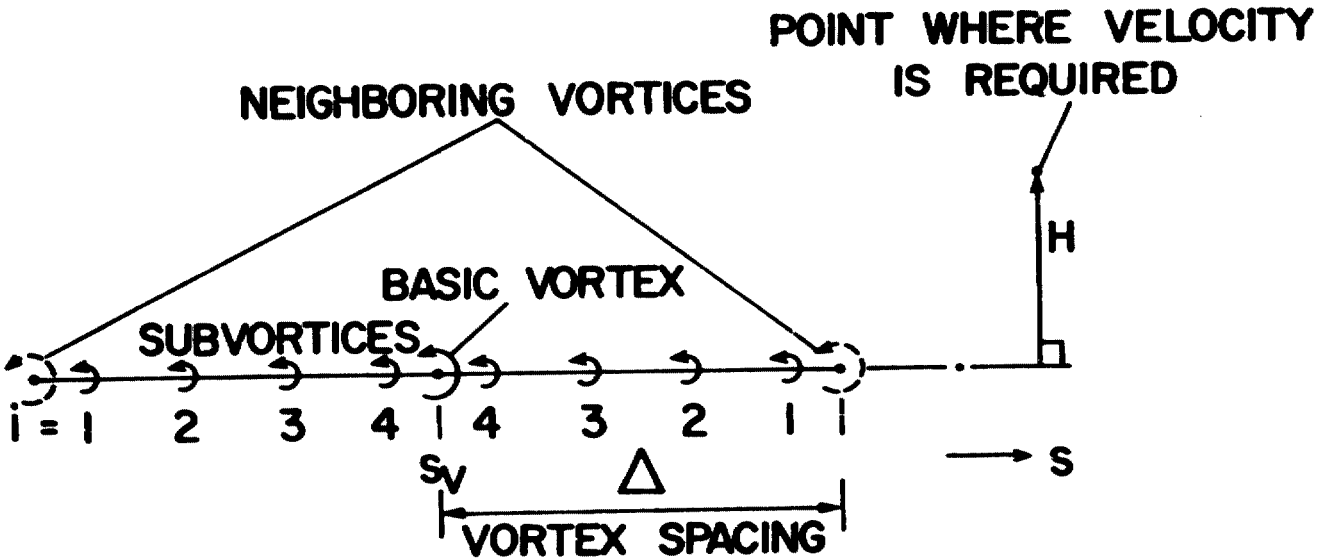

$$\text{SUBVORTEX POSITIONS, } s_i = s_V \pm \{NSV + 0.5 - i\}\Delta/NSV$$

(a) Arrangement of the subvortices for NSV = 4.

Figure 4.- Subvortex technique.

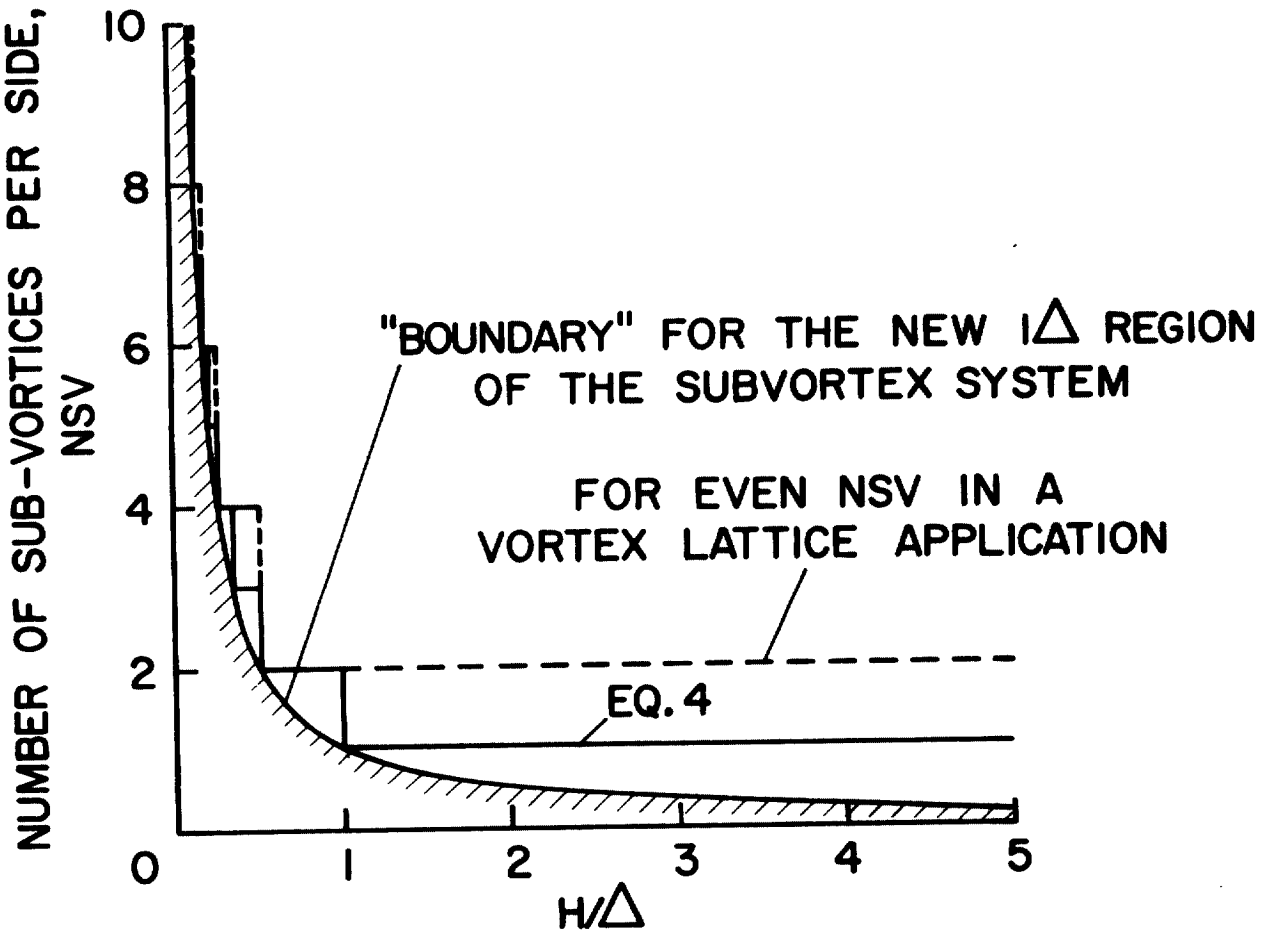

(b) Number of subvortices as a function of height above the segment.

Figure 4.- Concluded.

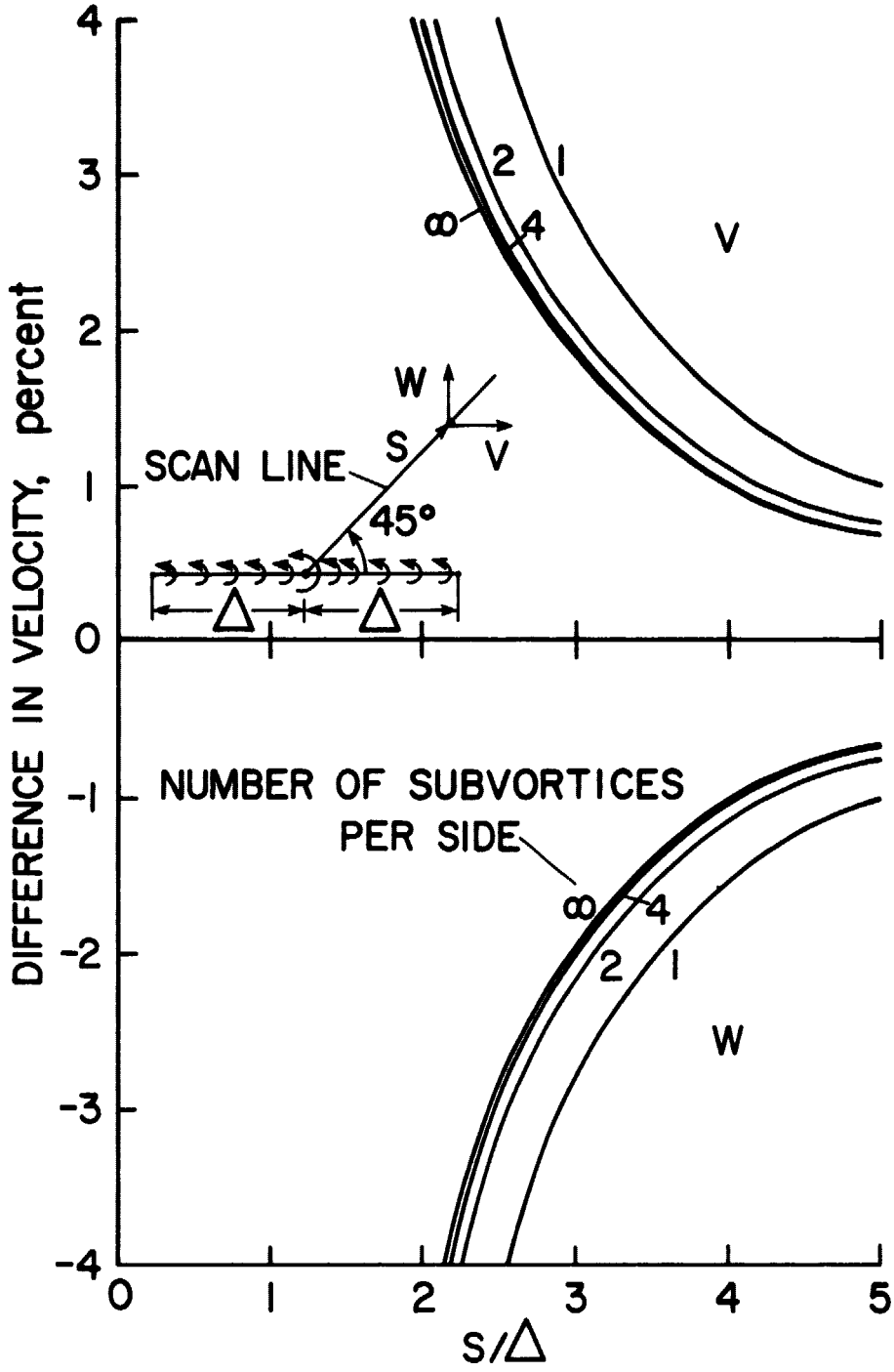

Figure 5.- Subvortex technique. Difference between velocities from subvortices and from the basic vortex.

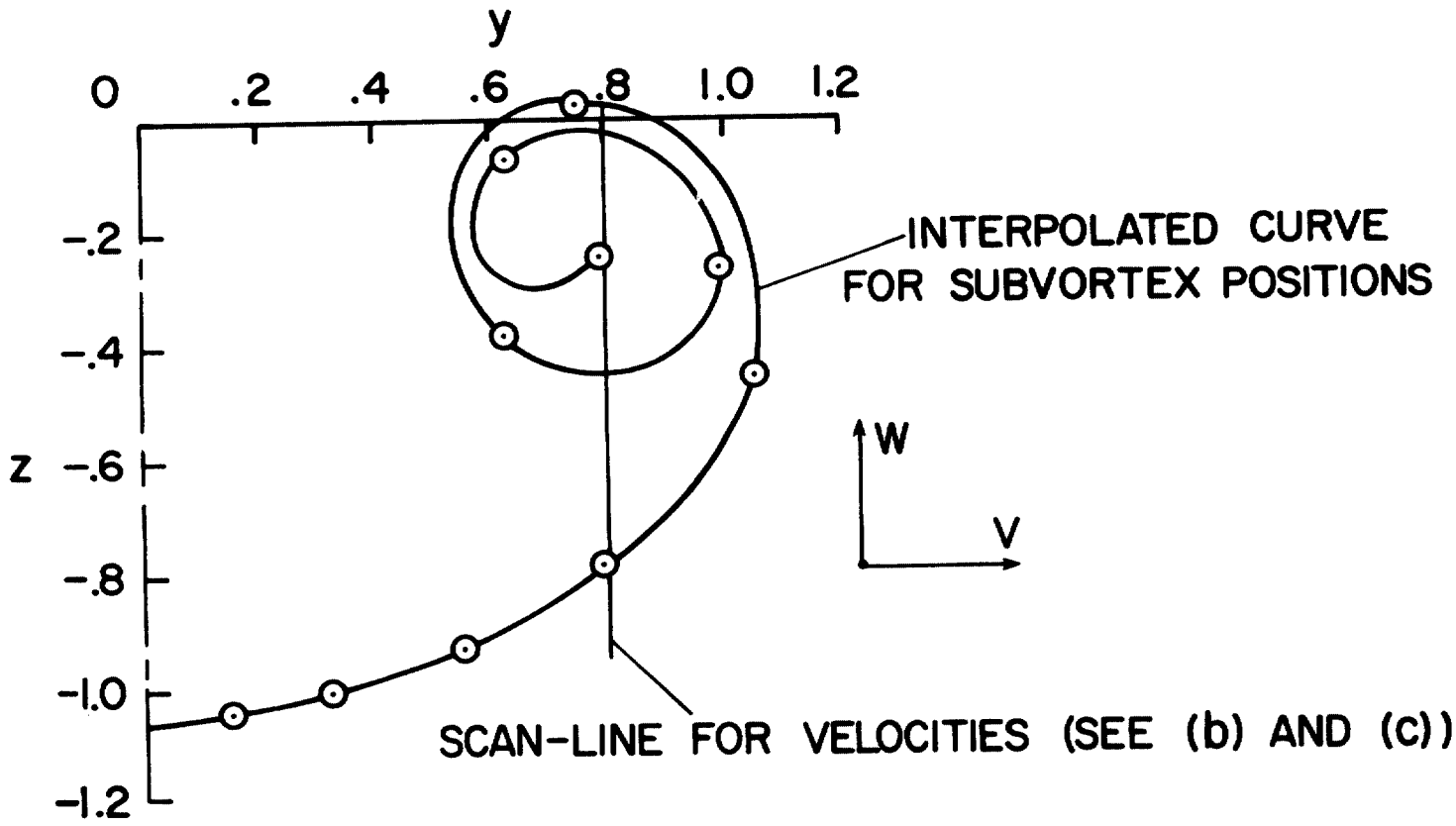

(a) Calculated vortex positions after 20 time steps (t = 1.5).

Figure 6.- Simple application of the subvortex technique to the vortex sheet roll-up calculation in two dimensions.

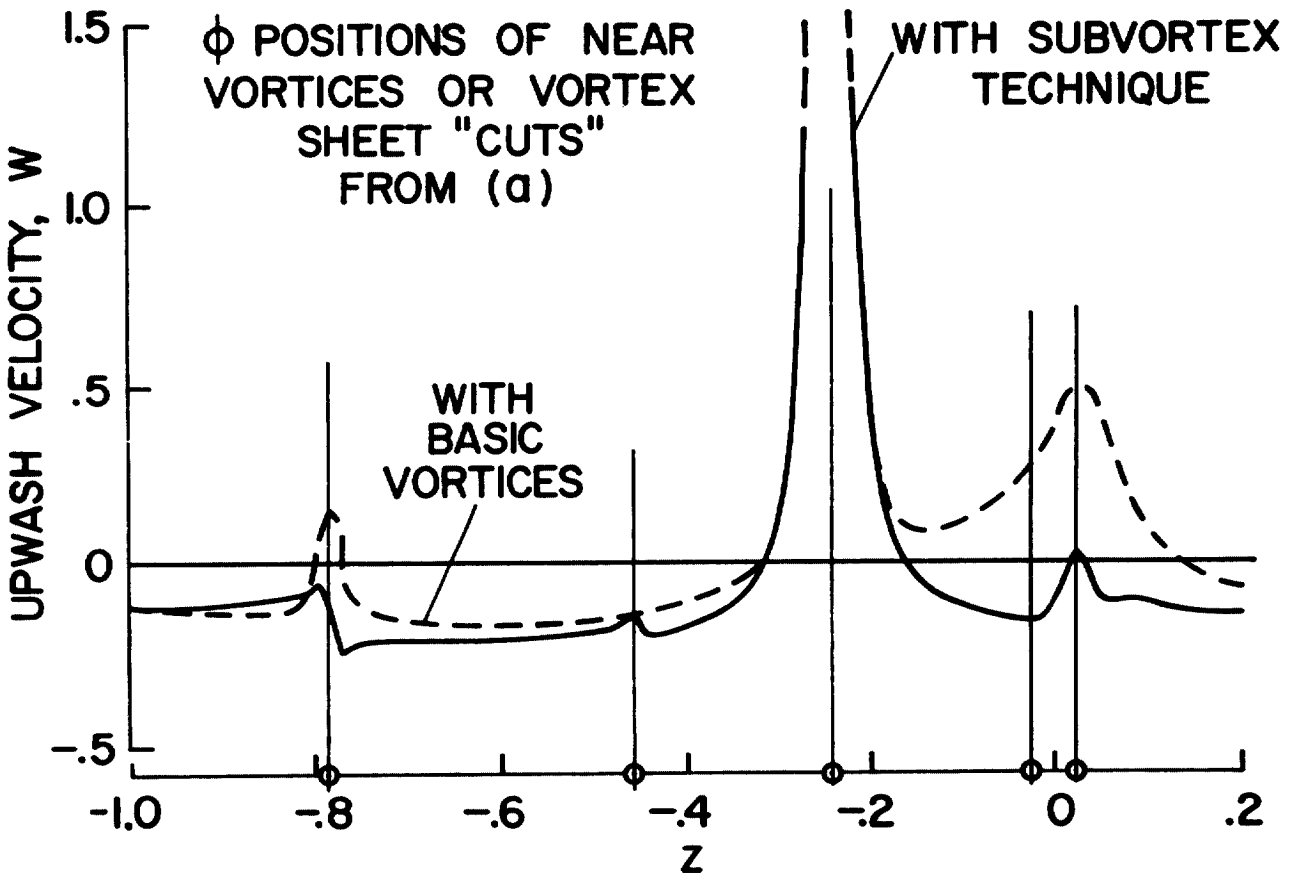

(b) Calculated upwash distribution.

Figure 6.- Continued.

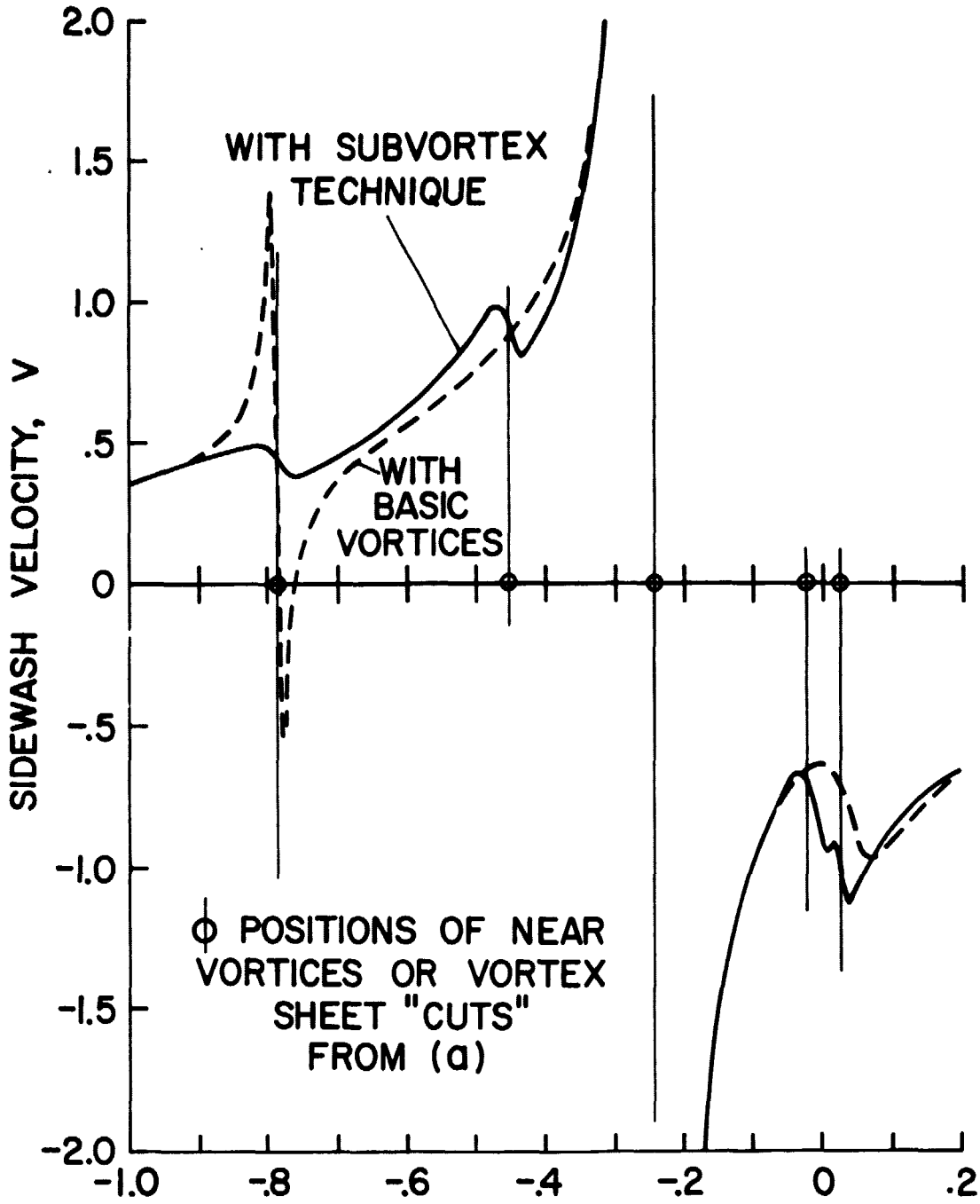

(c) Calculated sidewash distribution.

Figure 6.- Concluded.